Clusters in DMFT:
The case of M_1 phase of VO_2

1 Introduction

The $\mathcal{AMULET}$ package allows one to perform DMFT calculations for clusters constructed in real space. This cluster extension of DMFT (often called the CDMFT) can be used to take into account non-local correlation effects which are neglected in the conventional single-site DMFT (see, e.g., [1, 2]). In this case, a cluster is considered as an effective impurity in the Anderson model, and hence the intersite self-energy elements are introduced. The density functional theory (DFT) combined with the CDMFT was successfully applied to study real correlated compounds such as monoclinic phase of VO_2 [3, 4] and Ti_2O_3 [5], where the non-local effects within dimerized pairs of atoms play a crucial role. For these compounds, the single-site DMFT cannot reproduce the insulating state with physically reasonable values of Hubbard U.

In this Tutorial we consider the case of monoclinic M_1 phase of vanadium dioxide and demonstrate how to use the $\mathcal{AMULET}$ package for calculations within the DFT+CDMFT approach.

2 Crystal structure and DFT results

In the low-temperature M_1 phase, below 340 K, vanadium dioxide has a monoclinic crystal structure with space group $P2_1/c$ (details can be found in [6]). This structure is presented in Fig. 1 and can be viewed as distorted high symmetry rutile structure doubled along c_R axis (c axis of R phase). There is one type of vanadium atoms that are shifted to each other forming dimers tilted with respect to c_R direction. Each vanadium atom is surrounded by an oxygen octahedron resulting in a splitting of d level to triply degenerate t_{2g} and doubly degenerate e_g^σ states. Additional tetragonal distortion presented in the structure leads to further lifting of degeneracy of t_{2g} level to a_{1g} and π states. In the local coordinate system shown in Fig. 1 by (double) primed axes for vanadium atom, the local z' axis is chosen to be pointed to the apical oxygen atom, the local x' and y' are chosen to be pointed to the planar oxygens. Hence, a_{1g} state corresponds to the $d_{x'y'}$ orbital, π states to $d_{x'z'}$ and $d_{y'z'}$, e_g^σ states to $d_{z'^2}$ and $d_{x'^2-y'^2}$.

In order to calculate the electronic structure of M_1 phase within the local density approximation (LDA), the TB-LMTO method [7] was used. The obtained results are presented in Fig. 1 and have a good agreement with earlier studies [8]. The total density of states (DOS) is divided into three regions. The completely occupied part extends from -8 to -2 eV and is of oxygen character mostly. The middle region extended from -0.6 to 2.1 eV crosses the Fermi level and its partial character corresponds to the t_{2g} states of vanadium. The highest in energy part of DOS is separated by a small gap and is located in the energy range from 2.4 to 5.4 eV.

The dimerization of vanadium atoms leads to the well formed bonding-antibonding structure in a_{1g} partial DOS shown in the lower panel of Fig. 1. The bonding states are located just below the Fermi level (and partially cross it), while their antibonding counterparts are at 1.5 eV.
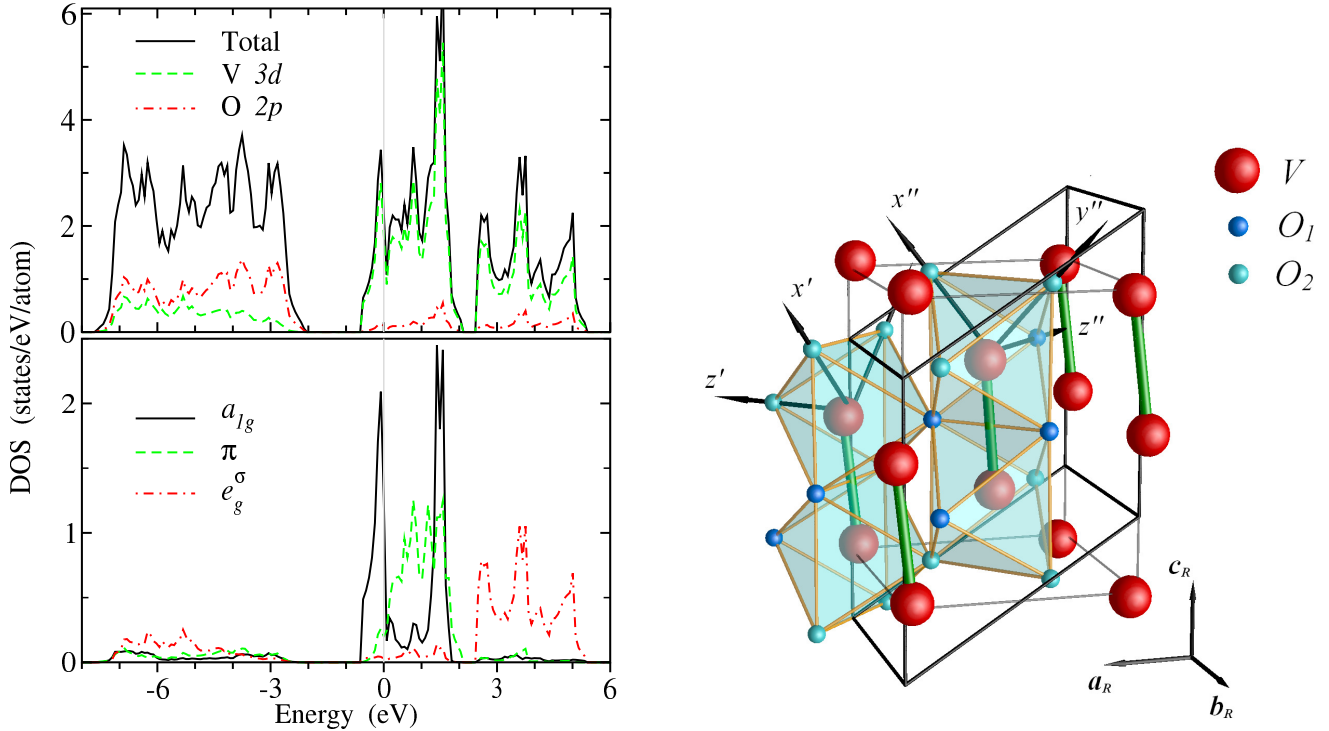
Figure 1: LDA density of states for M_1 phase (left panel). Top panel shows total, V $3d$, and O $2p$ DOSes by (black) solid, (green) dashed, and (red) dot-dashed lines, respectively. Bottom panel shows partial DOSes of different symmetry for a vanadium atom. The Fermi level is indicated by (grey) vertical line at zero energy. Crystal structure of monoclinic M_1 phase of VO_2 (right panel). (a_R, b_R, c_R) are rutile crystallographic axes. Local coordinate axes on the vanadium atoms are shown by (double) primed set.

Note that the LDA results in a metallic state. However, according to the experimental data, the M_1 phase is characterized by a band gap of about 0.6 eV (Ref. [9]).

The Hamiltonian matrix for the states near the Fermi level has been constructed using Nth-order muffin-tin orbital (NMTO) method [10]. Since the crystal-field splitting separates well the t_{2g} and e_g states, we include to the Hamiltonian matrix only three bands (t_{2g} symmetry mainly) from each V atom in the unit cell using the quadratic ($N = 2$) muffin-tin orbital set. In our case the unit cell contains four V atoms, and hence the obtained Hamiltonian matrix is of dimensions 12×12.

3 Input files for $\mathcal{AMULET}$

To start calculations with $\mathcal{AMULET}$ package, one can use the following **amulet.ini**.

```
Beta = 5
L = 20
ecut = 700
niter = 40
n_imp_type = 1
ntotal = 4
```

One can note that one type of impurity is required in our case. Now we proceed to the **impurity_1.ini** file. Let us use the value of the screened Coulomb interaction, U=4 eV, and the value of Hund's exchange, J=0.68 eV, from the earlier studies [3, 4]. When performing the cluster calculations, the Coulomb interaction matrix must be setup directly using token ummss. Note that introducing the Coulomb interaction via other tokens can lead to the nonphysical interaction. The token ummss introduces a matrix of size $2 * nlm$, which has a form

$$\begin{pmatrix} \widetilde{U}_{\uparrow\uparrow} & \widetilde{U}_{\uparrow\downarrow} \\ \widetilde{U}_{\downarrow\uparrow} & \widetilde{U}_{\downarrow\downarrow} \end{pmatrix},$$

where $\widetilde{U}_{\sigma\sigma\prime}$ is a matrix of size nlm containing Coulomb interaction values for particles with spin σ and $\sigma\prime$. Hence, the easiest way to make a ummss matrix for a cluster calculation is to add zero blocks to the ummss matrix taken from **amulet.out** in the single-site calculation with the same U and J.

The **impurity_1.ini** for the M_1 phase should look like this:

```
name = V

nlm = 6
n_imp = 2
himppos = 1 7

solver = 'HF-QMC'
nqmc = 2000000

Ummss =    0.00 1.96 1.96 0.00 0.00 0.00   4.00 2.64 2.64 0.00 0.00 0.00  \
           1.96 0.00 1.96 0.00 0.00 0.00   2.64 4.00 2.64 0.00 0.00 0.00  \
           1.96 1.96 0.00 0.00 0.00 0.00   2.64 2.64 4.00 0.00 0.00 0.00  \
           0.00 0.00 0.00 0.00 1.96 1.96   0.00 0.00 0.00 4.00 2.64 2.64  \
           0.00 0.00 0.00 1.96 0.00 1.96   0.00 0.00 0.00 2.64 4.00 2.64  \
           0.00 0.00 0.00 1.96 1.96 0.00   0.00 0.00 0.00 2.64 2.64 4.00  \
           4.00 2.64 2.64 0.00 0.00 0.00   0.00 1.96 1.96 0.00 0.00 0.00  \
           2.64 4.00 2.64 0.00 0.00 0.00   1.96 0.00 1.96 0.00 0.00 0.00  \
           2.64 2.64 4.00 0.00 0.00 0.00   1.96 1.96 0.00 0.00 0.00 0.00  \
           0.00 0.00 0.00 4.00 2.64 2.64   0.00 0.00 0.00 0.00 1.96 1.96  \
           0.00 0.00 0.00 2.64 4.00 2.64   0.00 0.00 0.00 1.96 0.00 1.96  \
           0.00 0.00 0.00 2.64 2.64 4.00   0.00 0.00 0.00 1.96 1.96 0.00
```

To capture the dynamical effects within a cluster, the non-diagonal elements of Green function matrix must be calculated by quantum impurity solver. For this purpose we use the Hirsch-Fye quantum Monte-Carlo (QMC) solver.

As the self-consistency is reached, one can find the next occupancy matrix in **amulet.out**:

```
   ...
   ...
  Occupation matrix for impurity #  1

  Spin    1
     0.31905    -0.01336     0.00285     0.19527    -0.00102    -0.00263
    -0.01336     0.07659    -0.01438    -0.00098    -0.01606    -0.01268
```

```
     0.00285    -0.01438     0.10428    -0.00256    -0.01272    -0.02118
     0.19527    -0.00098    -0.00256     0.31818    -0.01331     0.00277
    -0.00102    -0.01606    -0.01272    -0.01331     0.07729    -0.01458
    -0.00263    -0.01268    -0.02118     0.00277    -0.01458     0.10462
 Number of electrons in spin channel        1.00000042
 Number of electrons per impurity        2.00000084
  ...
```

One can clearly see the substantial intersite occupancy of 0.19527 for the a_{1g} states, while the other intersite elements are much smaller.

The DFT+CDMFT results for the magnetic and spectral properties of M_1 phase of VO_2 can be found in [3, 4].

References

[1] M. H. Hettler, A. N. Tahvildar-Zadeh, M. Jarrell, T. Pruschke, and H. R. Krishnamurthy, Phys. Rev. B **58**, R7475(R) (1998).

[2] A. I. Lichtenstein and M. I. Katsnelson, Phys. Rev. B **62**, R9283 (2000).

[3] S. Biermann, A. Poteryaev, A. I. Lichtenstein, and A. Georges, Phys. Rev. Lett. **94**, 026404 (2005).

[4] A. S. Belozerov, M. A. Korotin, V. I. Anisimov, and A. I. Poteryaev, Phys. Rev. B **85**, 045109 (2012).

[5] A. I. Poteryaev, A. I. Lichtenstein, and G. Kotliar, Phys. Rev. Lett. **93**, 086401 (2004).

[6] J. M. Longo and P. Kierkegaard, Acta Chem. Scand. **24**, 420 (1970).

[7] O. K. Andersen and O. Jepsen, Phys. Rev. Lett. **53**, 2571 (1984); O. K. Andersen, Z. Pawlowska, and O. Jepsen, Phys. Rev. B **34**, 5253 (1986).

[8] R. M. Wentzcovitch, W. W. Schulz, and P. B. Allen, Phys. Rev. Lett. **72**, 3389 (1994); M. A. Korotin, N. A. Skorikov, and V. I. Anisimov, Phys. Met. Metallogr. **94**, 17 (2002); V. Eyert, Ann. Phys. **11**, 650 (2002).

[9] T. C. Koethe, Z. Hu, M. W. Haverkort, C. Schuler-Langeheine, F. Venturini, N. B. Brookes, O. Tjernberg, W. Reichelt, H. H. Hsieh, H.-J. Lin, C. T. Chen, and L. H. Tjeng, Phys. Rev. Lett. **97**, 116402 (2006).

[10] O. K. Andersen and T. Saha-Dasgupta, Phys. Rev. B **62**, 16219 (2000).